UCRL-JC-131213
PREPRINT

Laser-induced damage of absorbing and diffusing glass surfaces under IR and UV irradiation

P. K. Whitman
K. Bletzer
J. L. Hendrix
F. Y. Génin
M. Hester
J. Yoshiyama

This paper was prepared for submittal to the
30th Boulder Damage Symposium: Annual Symposium on
Optical Materials for High Power Lasers
Boulder, Colorado
September 28 - October 1, 1997

December 22, 1998

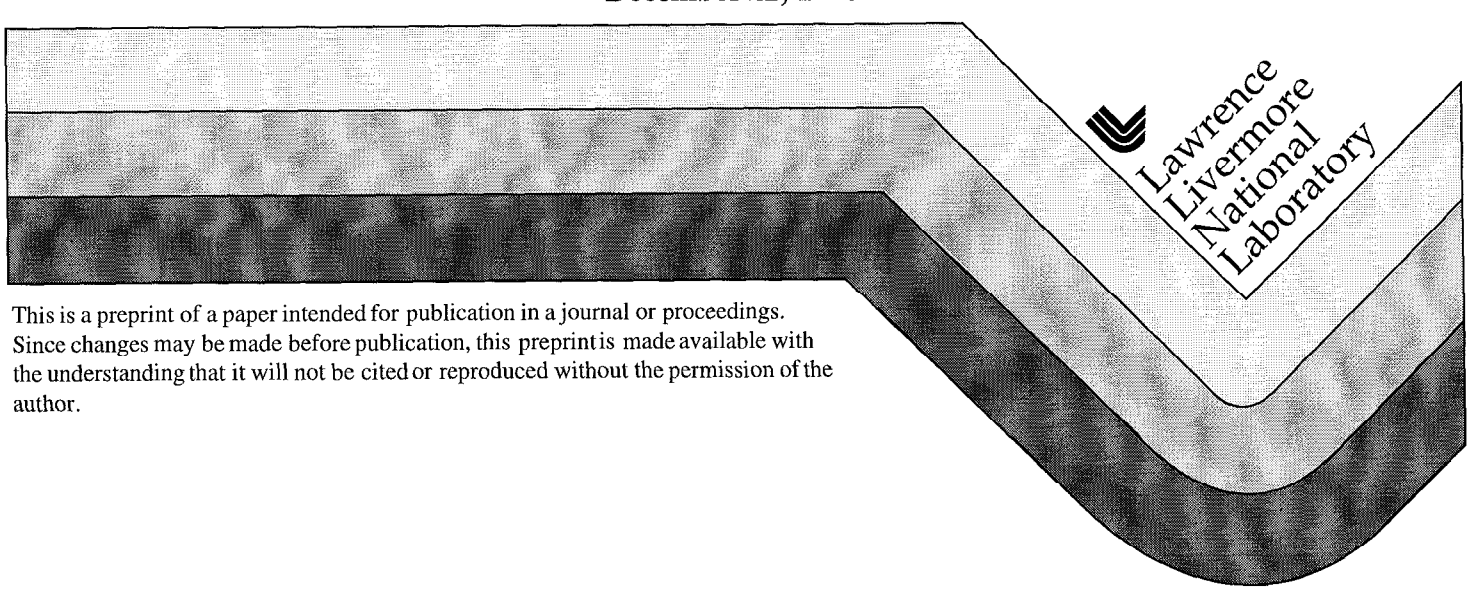

Laser-induced damage of absorbing and diffusing glass surfaces under IR and UV irradiation

P. K. Whitman, K. Bletzer, J. L. Hendrix, F. Y. Génin, M. Hester, and J. Yoshiyama

Lawrence Livermore National Laboratory
Livermore, CA 94551

ABSTRACT

In high peak power lasers used for inertial confinement fusion experiments, scattered and reflected light can carry sufficient energy to ablate metal structures or even damage other optics. Absorbing and diffuse scattering materials are required to manage the "ghosts", stimulated Raman scattering (SRS) and unconverted light in the laser chain and target chamber. Absorbing and diffuse scattering glasses were investigated for use in the NIF target chamber to safely dissipate up 60 – 80 J/cm^2 1053-nm light while also withstanding up to 2 J/cm^2 of soft x-ray. In addition these glasses were evaluated for use at 1053-nm and 351-nm to dissipate stray light and to absorb stimulated Raman scattering from the conversion crystals. Glass samples with surfaces ranging from specular to highly scattering (etched, sandblasted) were evaluated. The morphologies of laser damage at 1064 nm and 355 nm were characterized by Nomarski optical microscopy. Laser damage was quantified by measuring mass loss. Surface treatment and bulk absorption coefficient were the two material properties most strongly correlated to laser damage. Etched and sandblasted surfaces always had lower damage threshold than their specular counterparts. Reducing rear surface fluence either by bulk absorption or scattering at the input surface delayed the onset of catastrophic failure under extreme (60 J/cm^2) conditions.

Keywords: laser-induced damage, beam dump, surface morphology, absorbing glass, 355 nm, 1064 nm.

1. INTRODUCTION

Management of stray and unconverted light is essential to the safe and cost-effective operation of high energy, high peak power lasers such as the 192-beam system designed for the National Ignition Facility (NIF). "Beam dumps" are typically employed to absorb the unwanted stray or unconverted light. In the NIF laser design, the management of ghost reflections in the tightly packed final optics package and the management of the unconverted light in the target chamber present the two most challenging "beam dump" applications[1].

The final optics package contains the KDP conversion crystals, the final focusing lens, the diffractive optic structures for separating the converted and unconverted light and for smoothing the beam, and a fused silica debris shield. The debris shield is the interface between the final optics package and the target chamber. For a prototypical inertial confinement experiment where 1.8MJ of 351-nm light is focused on the target, an additional 1.2MJ of 1053-nm and 525-nm light must be safely dissipitated in the target chamber. The beam dumps in the target chamber must be designed to absorb or scatter peak fluences of 60 – 80 J/cm^2, 20ns mixed color laser light in the presence of up to 2 J/cm^2 200- 350 eV blackbody temperature x-rays without possibility of catastrophic failure nor introduction of collateral damage to the laser optics. The survival of the debris shield in the presence of contamination produced by targets, target chamber beam dumps and ablation of the target chamber wall helps define the allowable laser ablation of the target chamber beam dumps[2].

The debris shield serves as a sacrificial optic to isolate the more expensive optics in the final optics package from target chamber contamination. Ghost mitigation is a second crucial design consideration to prevent contamination-induced damage of the final optics[3,4] by laser ablation of metal structures in the final optics package. Ghosts are beams generated by reflections off optic surfaces. The final optics package contains 14 optic surfaces, including three gratings, which diffract significant fluences of red, blue, and green light into several orders. Hence, there are over a million ghosts with sufficient energy to ablate structural materials. Since many of the ghost reflections meet mechanical surfaces at near grazing angles, diffuse scattering materials are preferred to dissipate the energy rather than specular absorbing glass. Ghost reflections up to 2.2 J/cm^2, 3ns of combined 1053-nm, 531-nm, and 351-nm light are expected in the final optics assembly.[5]

2. OBJECTIVE

The objective of this work was to evaluate options for glass beam dump materials with potential for use in the management of unconverted light in the target chamber and ghost reflections in the final optics assembly. Materials are required which will not fail catastrophically, will not generate contamination which could limit the lifetime of the final UV laser optics, and that are cost effective for the large areas required in the target chamber or final optics assemblies.

3. PERFORMANCE AT 1053-NM

Earlier work[1] demonstrated a strong correlation between the thermal expansion coefficient and the mass loss of a glass coupon subjected to the x-ray fluences expected at the target chamber wall. This was due to thermal crazing and subsequent massive spallation for high thermal expansion materials such as soda-lime glasses. Glass compositions with thermal expansion less than $6x10^{-6}$ per °C behaved nominally the same as fused silica and were deemed acceptable for use in the target chamber. But these undoped materials failed to absorb sufficient 1053-nm absorption to prevent the unconverted light from ablating the target chamber wall and beam dump support structures, and hence were expected to suffer catastrophic laser damage. Appropriately doped optical filter glasses and architectural glasses met the laser damage criteria, but had high thermal expansion and failed the x-ray ablation criteria. To meet our cost objectives, we wished to utilize commercially available glasses rather than develop a new material. Hence, we evaluated a sandwich concept for the target chamber beam dumps where the first substrate absorbed the x-ray fluence but transmitted the laser light and the second substrate had only to absorb the laser fluence. Three sets of experiments were conducted to first screen and then quantify performance of potential candidates for glass target chamber beam dumps. Performance of the best glass beam dump materials was then compared against other candidate materials such as stainless steel and boron carbide.[1,6,7]

3.1 SCREENING EXPERIMENTS

Screening experiments were conducted in air using a focused, small Gaussian beam ($0.1mm^2$) Nd:YAG laser at 1064 nm[8]. The first set of experiments was conducted at near normal incidence (15°), 60 J/cm^2, 9.7ns, 10 Hz repetition rate. Damage was qualitatively assessed using Nomarski optical microscopy. Qualitative rankings of these glasses are shown in Table 1. Absorbing glass compositions generally had better laser damage performance than the transparent glasses, independent of whether they were tested with as-received (specular) or as diffusely scattering surfaces. Transparent glass performed better with diffusely scattering surfaces than specular surfaces.

Commercial and optical glasses with low absorption coefficients (< 0.5 cm^{-1}) were also tested with either specular or diffusely scattering surfaces. Sandblasted or Blanchard ground surfaces effectively scattered rather than absorbed much of the unconverted light and delayed the onset of catastrophic damage. Sandblasted samples typically failed catastrophically after 100 – 300 shots, regardless of whether they were near-optical quality fused silica or inexpensive borosilicate float glass. Figure 1a shows the typical 'catastrophic' damage morphology.

For absorbing glass, it was proposed that catastrophic laser damage could be avoided by limiting the surface temperature rise of the glass. Since the laser pulse is short with respect to the rate of thermal diffusion, a simple model can be used to estimate the single shot surface temperature increase based upon the heat capacity (C_p), density (ρ), and absorption coefficient of the glass (α) and the pulse fluence (F) at the test wavelength:

$$\Delta T = (\alpha F)/(\rho C_p) \quad (1)$$

Architectural glasses with absorption coefficients between 1.5 – 3 cm^{-1} at 1-μm were chosen to limit the surface temperature rise to less than 150°C at 60 J/cm^2. Catastrophic damage was not observed for either specular (as-received float glass) or sandblasted absorbing glasses. Figure 1b shows the typical 'melted surface' damage morphology that developed after multiple shots at high fluence, even though the calculated single shot surface temperature was well below the melting point of the glass. PPG Azurlite® architectural glass, a blue glass with 1-μm absorption coefficient of 3.7 cm^{-1} was selected as the most promising material for further testing.

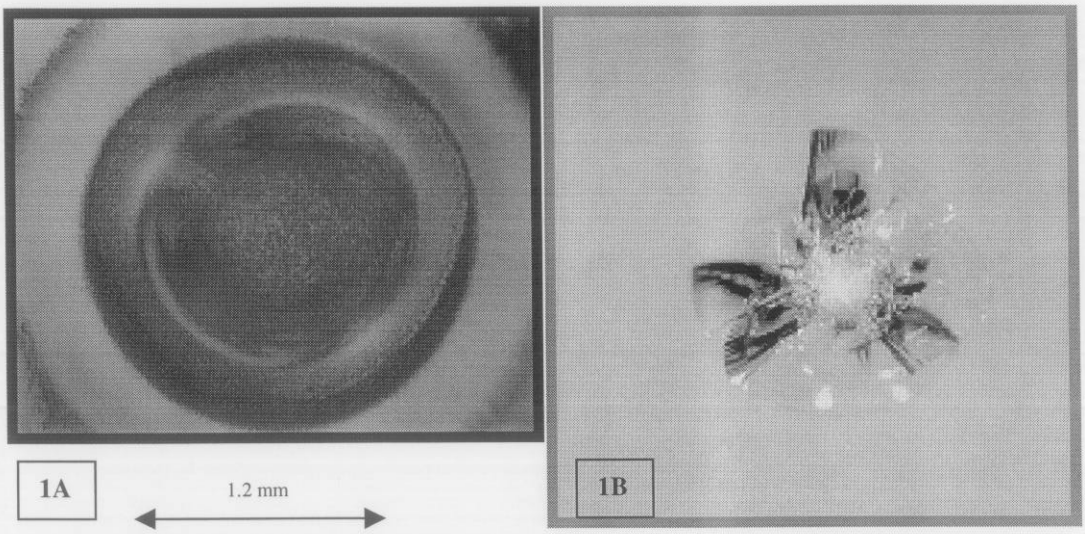

Figure 1: Comparison of the melt damage morphology characteristic of absorbing glasses with the catastrophic damage morphology observed for transparent glasses. 1a) melt damage in as-received PPG Azurlite® blue architectural glass. 1b) Catastrophic damage developing in as-received Schott Borofloat™ glass. Each sample was photographed after 30 shots at 60 J/cm2, 10 Hz.

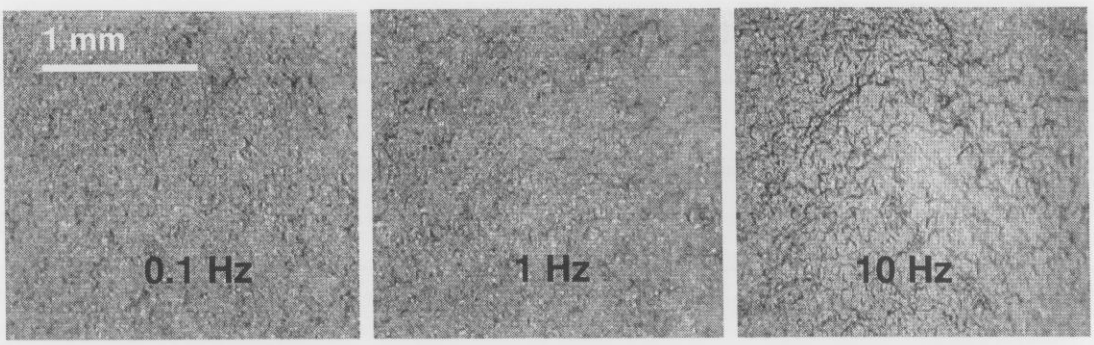

Figure 2a: Surface roughening increased with increasing repetition rate for sandblasted Azurlite® absorbing glass. All samples were photographed after 100 shots, 60J/cm^2

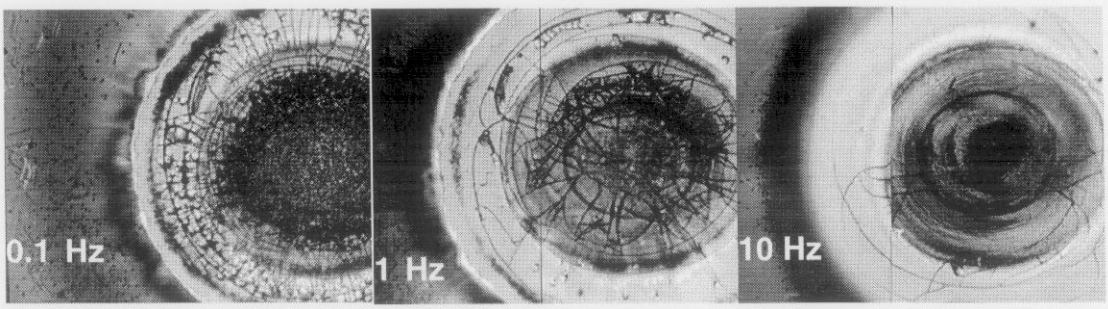

Figure 2b: The melt diameter increases and the thermal crazing decreases with increasing shot repetition rate for as-received Graylite® absorbing glass. b) Surface roughening increased with increasing repetition rate for sandblasted Azurlite® absorbing glass. All samples were photographed after 100 shots, 53 J/cm^2.

Table 1: Results of small beam laser damage and Nova x-ray ablation tests. Laser damage rankings are reported for 600 shots, 60 J/cm^2, 0.8 mm beam, in air. Approximate x-ray ablation rates are reported relative to the ablation rate of fused silica. Low thermal expansion materials give low x-ray ablation.

	Absorption Coefficient at 1053-nm (per cm)	Specular Surface Laser Damage Performance	Sandblasted Surface Laser Damage Performance	Thermal Expansion Coefficient (x 10^6)	X-ray Ablation Comparison (FS = 1)
Doped Glasses					
PPG Azurlite®	3.7	Good	Good	8.6	10
PPG Solex®	2.9	OK	Good	8.6	10
PPG Graylite® 14	1.6	Good	Good	8.6	10
Undoped Glasses					
Fused Silica (FS)	0	Fail	OK	0.6	1
Schott Borofloat™ borosilicate	0.1	Fail	OK	3.3	2
Corning Pyrex™ borosilicate	0.1	Fail	OK	3.3	2
Schott VG-10	0.8	Good	Good	11.0	20
Schott BK-7	0	Fail	OK	7.4	10

A second set of screening experiments explored the effect of repetition rate and angle of incidence. These experiments were conducted in air at 53 J/cm^2, 3.5ns, in air and at 60 J/cm^2, 9.7ns. Repetition rate was varied from 0.1 to 10 Hz and the angle of incidence was tested at near normal (10°) and 45°. These results are summarized in Table 2. Increasing the angle of incidence generally reduced laser damage at the lower repetition rates, but had no effect at 10 Hz. Increasing the repetition rate from 0.1 to 10Hz produced greater damage for both absorbing and diffusing glasses.

Figures 2a and b contrast the increased roughening which developed on sandblasted absorbing glass with the increase in melt diameter and decrease in thermal crazing which occurred on the as-received float glass as the repetition rate was increased. Although there was no qualitative transformation of damage morphology (samples which melted at low repetition rate did not fail catastrophically at high repetition rate or vice versa), the damage extent and morphology is clearly dependent upon repetition rate. The energy absorbed in a 1 cm thick sample of absorbing glass can be estimated from the exponential function:

The effect of repetition rate on bulk temperature rise can be estimated as follows. The temperature increase from a single shot can be calculated from the energy absorbed into the thickness, x, of the sample.

$$\Delta T = F(1-e^{-\alpha x})/x\rho C_p \qquad (2)$$

For a small beam, the diffusion path length, L, can be estimated from the diffusivity, D and the diffusion time, τ:

$$L = \sqrt{4D\tau} \qquad (3)$$

Between shots, the absorbed heat is dissipated into a volume $\pi L^2 x$. The temperature rise from shot to shot is then directly proportional to the square of the diffusion length divided by the beam radius. As τ, the time elapsed between shots, increases, the steady state temperature rise decreases. For Azurlite® absorbing glass, the calculated temperature exceeds the melting point of the glass after a few hundred shots at 10 Hz, but remains essentially at ambient temperature at 0.1Hz shot rate and increases only some 50 °C after 600 shots at 1 Hz. This is consistent with the reported observations for sandblasted absorbing glasses. Since the NIF laser will be fired only once every 4 – 8 hours, artifacts due to high repetition rates could result in erroneously accepting or rejecting a borderline material.

3.2 ESTIMATION OF LASER ABLATION RATES

In order to quantitatively compare the performance of the most promising target chamber beam dump materials, it was necessary to calculate mass generation curves as a function of fluence. The experiments were run in vacuum at 10^{-5} torr using a 3mm x 4mm beam generated by the Advanced Glass High Average Power (AGHAP) laser at LLNL. The 1053-nm, 14-ns FWHM Gaussian beam was pulsed at 0.1Hz for the glass samples – a compromise between introducing non-representative thermal effects in the absorbing glass and completing the experiments within a reasonable timeframe. All of the candidate glass materials were tested at normal incidence, both as individual pieces and in the proposed 'sandwich' configuration. A subset of these experiments was repeated at 60 J/cm^2, 14-ns in air at atmospheric pressure.

Figures 3 and 4 summarize the observed mass loss data for absorbing and non-absorbing glasses. Mass loss per shot is calculated by dividing the total mass loss by the number of shots, hence assuming that the damage rate was constant for all shots. This appears to be a good assumption for absorbing glass,

Table 2: Damage after 100 shots as a function of repetition rate and angle of incidence was qualitatively evaluated on a scale of 0 – 10. 1 denotes mild surface discoloration, 3 is minor surface cracking or melting, and 5 is a large amount of melting or surface damage. Samples denoted 'SB' had sandblasted surfaces.

Fluence, incidence angle	53 J/cm^2, 15° AOI			60 J/cm^2, 10° AOI			60 J/cm^2, 45° AOI		
Repetition rate	0.1 Hz	1 Hz	10 Hz	0.1 Hz	1 Hz	10 Hz	0.1 Hz	1 Hz	10 Hz
Azurlite®	2	3	3	0	0	4	0	0	0
Azurlite®, SB	2	2	3	2	3	4	1	1	4
Graylite®	1	1	1	1	1	4	1	1	4
Graylite®, SB	2	2	3	3	3	4	1	2	4
Borofloat™, SB	-	-	-	-	-	-	0	0	5
Fused Silica, SB	-	-	-	2	3	4	0	0	5

which never damaged catastrophically. The Azurlite® ablation rate appears to increase exponentially with fluence throughout the test range. For the fused silica and borosilicate glass, catastrophic damage occurred somewhat unpredictably, generally between 100 and 500 shots, making the estimation of mass generation less certain. Sandwiches of fused silica and Azurlite® did not noticeably reduce the damage to the fused silica input surface, but they did eliminate ablation from the Azurlite® surface at even the highest fluence. Figure 5 compares the morphology for specular and sandblasted absorbing glass after 500 shots in air or vacuum. The absorbing glass produces a very regular melted imprint of the beam with a halo of ablation products when damaged in air. In vacuum, the absorbing glass damage site is less regular and the mass lost is roughly four times higher. Figure 6 compares Blanchard ground fused silica and sandblasted borosilicate glass, which are damage tested in air and vacuum. Once again, the damage spot is larger and less regular in vacuum vs. air and the mass loss increases in vacuum. Any difference in performance between fused silica and borosilicate could not be distinguished from part-to-part variability. An additional set of tests was conducted on sandblasted fused silica to evaluate the potential for a louvered glass beam dump design. In this design, the fused silica louvers would be mounted at 45 – 60° angle of incidence while the absorbing glass would remain normal to the beam. As seen in Figure 7, the higher angle of incidence may delay the onset of catastrophic damage, but the data is too sparse and scattered to draw firm conclusions. In this configuration, the edges of the sample that faced the beam at near normal incidence damaged extensively. This is a primary concern for louvered glass beam dumps.

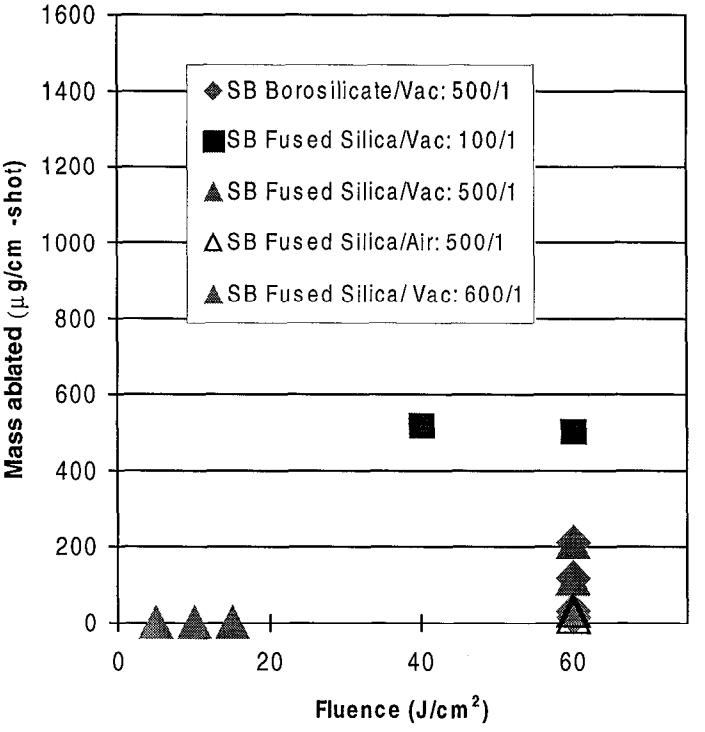

Figure 3: Mass generation for sandblasted borosilicate and fused silica tested at 0.1Hz, near normal incidence. Calculations are the average of 500 shots in vacuum, unless otherwise indicated.

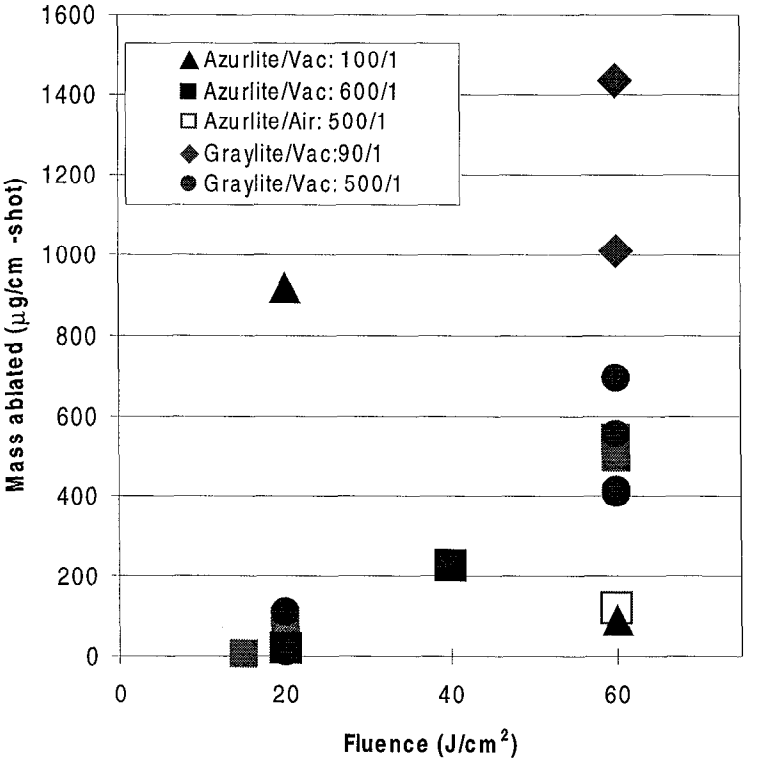

Figure 4: Mass generation for sandblasted absorbing glasses tested at 0.1Hz, near normal incidence. Calculations are the average of 500 shots in vacuum, unless otherwise indicated.

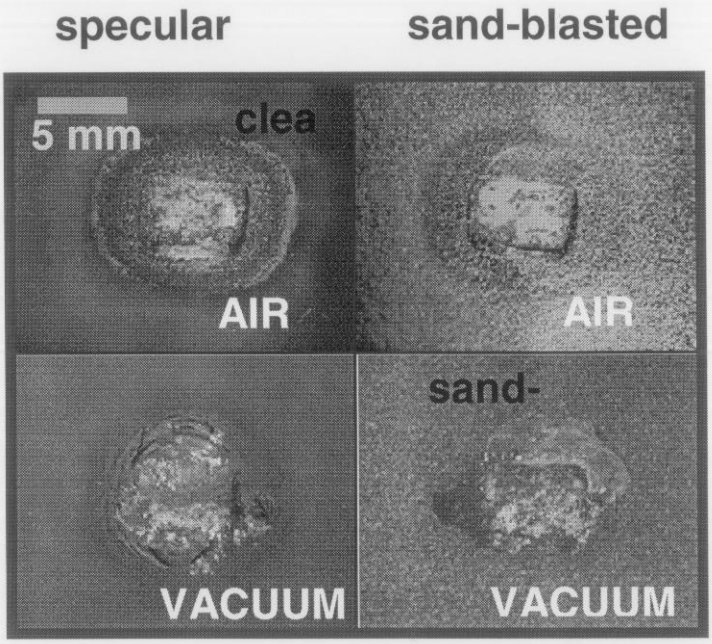

Figure 5: Comparison of sandblasted or specular Azurlite® absorbing glass damage after 500 shots in air or vacuum, 60 J/cm^2, 0.5 Hz.

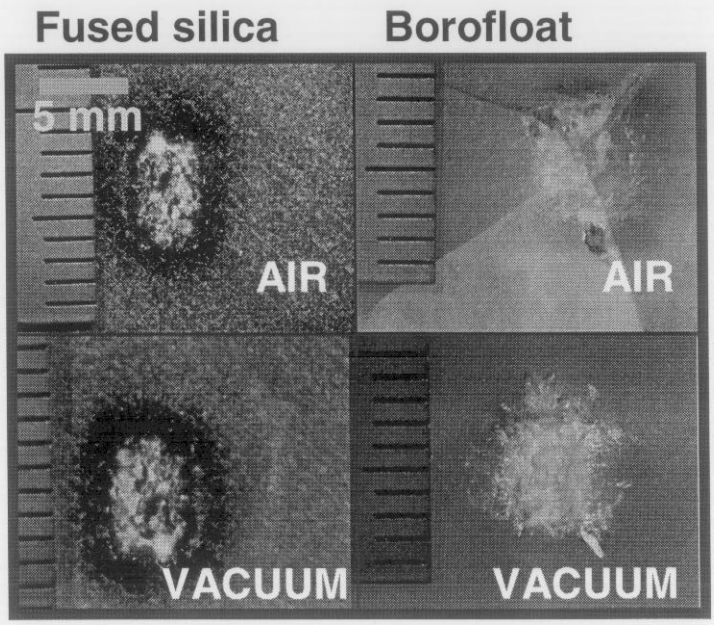

Figure 6: Comparison of sandblasted non-absorbing glass damage after 500 shots in air or vacuum, 60 J/cm^2, 0.5 Hz. (The large cracks in the Borofloat™ sample are mechanical fracture due to handling after the laser test, not laser damage.)

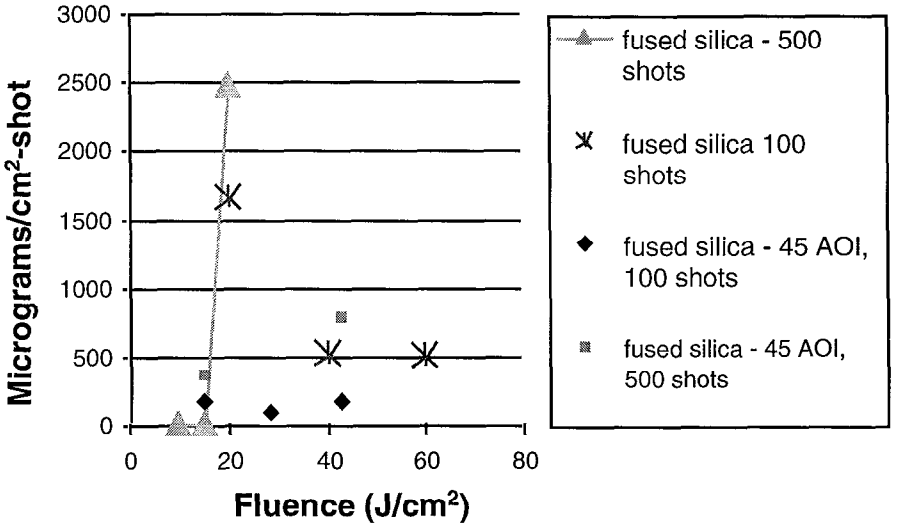

Figure 7: Sandblasted fused silica mass generation depends strongly on angle of incidence. Calculations are the average of 500 shots, unless otherwise indicated.

4. PERFORMANCE AT 351 NM

The first series of tests was designed to screen candidate materials based on particulate generation, plasma formation and initiation of visible damage. A subset of this series of experiments was designed to evaluate the impact of etching and sandblasting glass surfaces on the laser induced damage threshold (LIDT) as detected visually at 100x with a Nomarski microscope. A 355-nm Nd:YAG laser with Gaussian beam focused to 1.9mm, pulse length 8.4ns, at near normal incidence was utilized for these tests[9]. Tests were conducted at 1 Hz, and samples were examined after 1, 10 and 100 shots at the test fluence.

Since the onset of damage is difficult to perceive on diffuse samples, the functional LIDT was verified by the observation of particulate formation. A laboratory microscope slide was inserted between the test beam and the test sample after the first, 10^{th}, and 100^{th} shot to collect any particulate generated by laser damage. (The microscope slide transmitted > 85% of the 351-nm light.) All test samples were washed with alkaline detergent in an ultrasonic water before testing. Nevertheless, the first shot generally liberated surface contamination that had not been removed by the ultrasonic washing, thus making it difficult to establish the laser fluence where particulate contamination commenced.

Table 3 summarizes the LIDT for two architectural glasses after various surface treatments: 1) as-received, 2) sandblasted, 3)etched by a commercial HF process, 4) sandblasted and then solution etched by the commercial HF solution process, and 5) etched with a commercial etch paste. The LIDT for the as-received float glass is comparable to that of super-polished NG glass[9] and is approximately a factor of two higher than the LIDT for any of the processes which results in a diffuse surface. Figure 8 compares the damage morphologies for as received, solution etched, and sandblasted PPG Azurlite® architectural glass after 1 shot at 7 J/cm2. Figure 9 shows the Nomarski micrographs for solution etched Graylite® architectural glass after 1, 10, and 100 shots at the LIDT and the corresponding particle contamination collected on the microscope witness sample.

Table 4 compares the fluence where particulate formation was observed to the micrograph-derived LIDT for the various surface treatments. The particulate formation thresholds confirm the LIDT's measured by traditional methods, even though the various diffuse scattering surface treatments make detection of surface damage much more difficult compared to detection of damage on specular glass. Figure 10 compares the Nomarski micrograph for NitroSil® opaque fused silica to its corresponding the particulate witness slide at the 100/1 LIDT. The very rough surface of the Nitrosil® obscured any laser damage that occurred at lower fluences, and hence a falsely high LIDT was reported for this material.

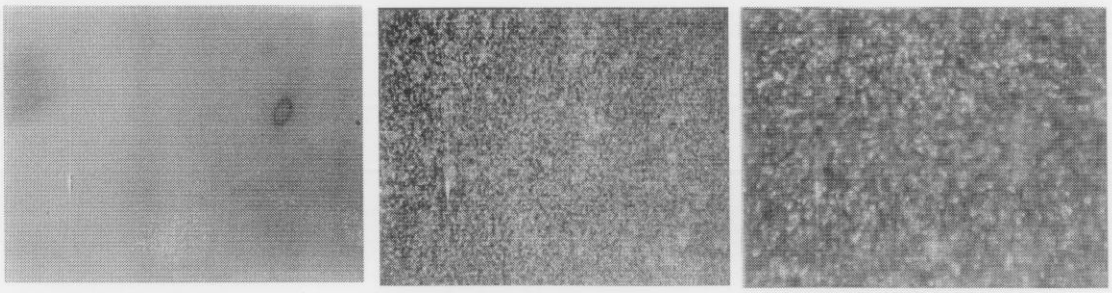

Azurlite as-received
1/1 LIDT 6.9 J/cm^2

Azurlite solution etched
1/1 LIDT 7.1 J/cm^2

Azurlite Sandblasted
1/1 LIDT 7.0 J/cm^2

Figure 8: Comparison of the damage morphologies for Azurlite® absorbing glass with three different surface treatments. All photographs are after a single shot at 7 J/cm2.

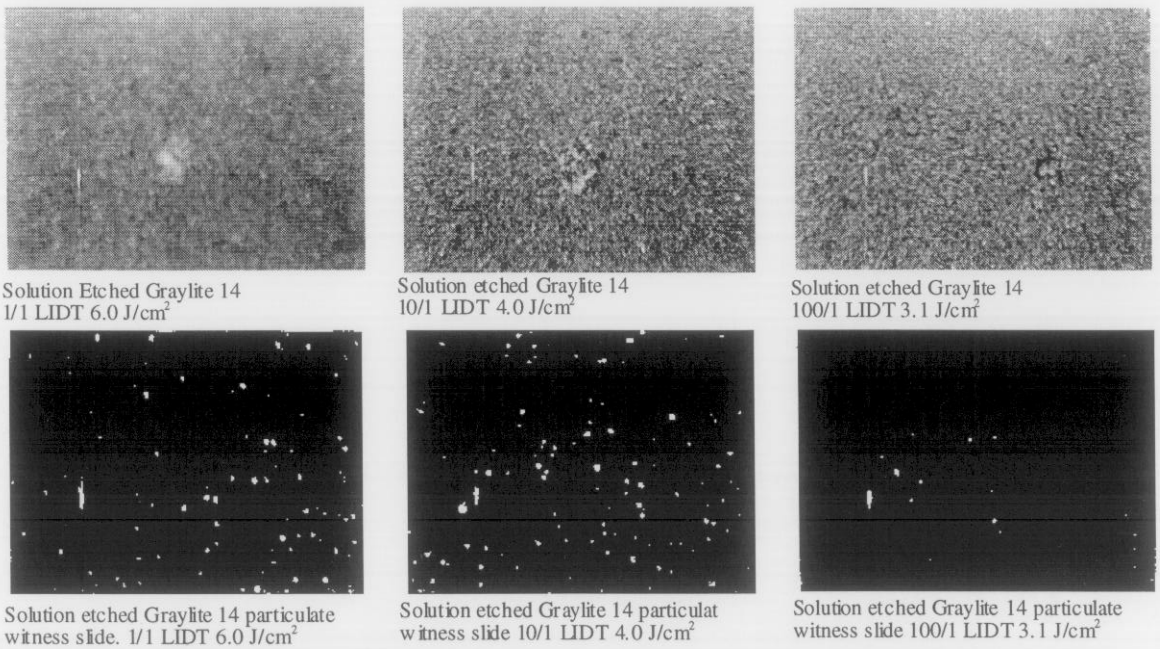

Solution Etched Graylite 14
1/1 LIDT 6.0 J/cm^2

Solution etched Graylite 14
10/1 LIDT 4.0 J/cm^2

Solution etched Graylite 14
100/1 LIDT 3.1 J/cm^2

Solution etched Graylite 14 particulate witness slide. 1/1 LIDT 6.0 J/cm^2

Solution etched Graylite 14 particulat witness slide 10/1 LIDT 4.0 J/cm^2

Solution etched Graylite 14 particulate witness slide 100/1 LIDT 3.1 J/cm^2

Figure 9: Correlation between the particulate formation and the damage morphologies after 1, 10 and 100 shots at the LIDT for Graylite® absorbing glass with solution etched surfaces.

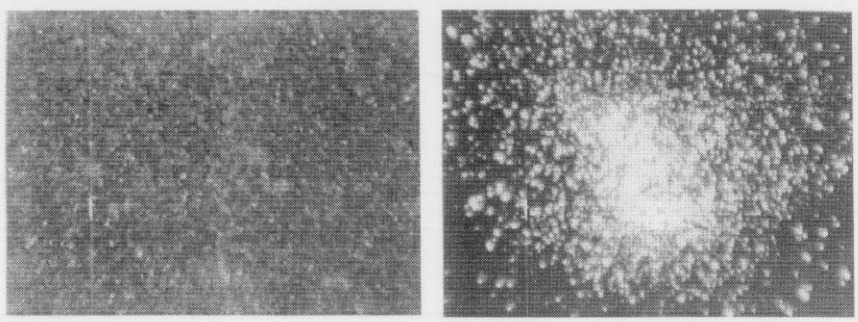

NitroSil™
100/1 LIDT 4.2 J/cm^2

NitroSil™ particulate witness slide
100/1 LIDT 4.2 J/cm^2

Figure 10: The surface of the NitroSil™ (left) appears undamaged after the 100th shot at the LIDT of 4.2 J/cm^2, but significant material was collected on the witness slide (right).

Table 3: The LIDT for PPG Azurlite® and Graylite® architectural glasses with specular (as-received) surfaces and after various treatments that create diffuse scattering surfaces.

PPG Azurlite®	*Damage Fluence J/cm² ±0. 5 J/cm²*	*1/1*	*10/1*	*100/1*
	As-received	6.9	6.1	5.1
	Sandblasted	7.0	3.2	2.0
	Sandblasted and Solution etched	5.1	3.6	2.5
	Solution Etched	7.1	4.2	2.8
	Paste Etched	6.2	2.5	1.8
PPG Graylite® 14				
	As-received	6.0	5.0	5.0
	Sandblasted	6.5	4.1	2.8
	Sandblasted and Solution etched	6.0	3.0	3.0
	Solution Etched	6.0	4.0	3.1
	Paste Etched	6.0	3.7	3.0

Table 4: The 351-nm fluence required to generate particles after 100 shots.

PPG Graylite 14	*Particulate Fluence J/cm² ±0.5 J/cm²*	*100/1 Particulate formation range*
	As-received	4.25 J/cm² —4.75 J/cm²
	Sandblasted	2.80 J/cm²— 4.15 J/cm²
	Sandblasted and Solution etched	No Data —3.05 J/cm²
	Solution Etched	3.00 J/cm²— 3.50 J/cm²
	Paste Etched	3.00 J/cm²— 3.75 J/cm²

4. SUMMARY

The operating conditions that are expected for the NIF target chamber beam dumps preclude utilization of a single commercial glass composition to simultaneously withstand the expected x-ray and laser fluences. Concepts that utilize a glass sandwich composed of a low thermal expansion glass to absorb the x-ray fluence backed by an absorbing glass to manage the laser fluence have been explored. In general, low absorption glasses fail catastrophically by brittle fracture while the absorbing glass experiences more benign melt damage. Sandblasting or otherwise reducing the specular transmission of low absorption glasses delays the onset of catastrophic output surface failure. Inexpensive architectural glasses can meet the 1053, 525, and 351-nm fluence and absorption requirements for the final optics assembly. The highest damage thresholds are achieved for the as-manufactured specular float glass surfaces. Etching, sandblasting, or a combination of etching and sandblasting the surface lowers the damage threshold by a factor of 2 – 3. The addition of witness plates to collect laser-ablated particulate in addition to traditional Nomarski microscopy LIDT tests enables the identification of the initiation of laser damage on rough surfaces.

ACKNOWLEDGMENTS

This work was performed under the auspices of the U. S. Department of Energy by Lawrence Livermore National Laboratory under Contract No. W-7405-ENG-48

REFERENCES

1. P. K. Whitman, A. K. Burnham, M. Norton, F.Y. Génin, J. M. Scott, W. Hibbard, K. Bletzer, A. T. Anderson, S. Dixit "Management of unconverted light for the National Ignition Facility target chamber," Solid State Lasers for Application to Inertial Confinement Fusion Third International Conference, June 7 – 12, 1998, Monterey, California.